ORIGINAL ARTICLE

EGFR Inhibition by Erlotinib Rescues Desmosome Ultrastructure and Keratin Anchorage and Protects against Pemphigus Vulgaris IgG–Induced Acantholysis in Human Epidermis

Desalegn Tadesse Egu[1,7], Thomas Schmitt[1,7], Nancy Ernst[2,3], Ralf Joachim Ludwig[2,3], Michael Fuchs[1], Matthias Hiermaier[1], Sina Moztarzadeh[1], Carla Sebastià Morón[1,4], Enno Schmidt[2,3], Vivien Beyersdorfer[5,6], Volker Spindler[5,6], Letyfee Sarah Steinert[1], Franziska Vielmuth[1], Anna Magdalena Sigmund[1,8] and Jens Waschke[1,8]

Pemphigus is a severe blistering disease caused by autoantibodies primarily against the desmosomal cadherins desmoglein (DSG)1 and DSG3, which impair desmosome integrity. Especially for the acute phase, additional treatment options allowing to reduce corticosteroids would fulfill an unmet medical need. In this study, we provide evidence that EGFR inhibition by erlotinib ameliorates pemphigus vulgaris IgG–induced acantholysis in intact human epidermis. Pemphigus vulgaris IgG caused phosphorylation of EGFR (Y845) and Rous sarcoma-related kinase in human epidermis. In line with this, a phosphotyrosine kinome analysis revealed a robust response associated with EGFR and Rous sarcoma-related kinase family kinase signaling in response to pemphigus vulgaris IgG but not to pemphigus foliaceus autoantibodies. Erlotinib inhibited pemphigus vulgaris IgG–induced epidermal blistering and EGFR phosphorylation, loss of desmosomes, as well as ultrastructural alterations of desmosome size, plaque symmetry, and keratin filament insertion and restored the desmosome midline considered as hallmark of mature desmosomes. Erlotinib enhanced both single-molecule DSG3-binding frequency and strength and delayed DSG3 fluorescence recovery, supporting that EGFR inhibition increases DSG3 availability and cytoskeletal anchorage. Our data indicate that EGFR is a promising target for pemphigus therapy owing to its link to several signaling pathways known to be involved in pemphigus pathogenesis.

Keywords: Desmogleins, EGFR signaling, Erlotinib, Pemphigus

Journal of Investigative Dermatology (2024) **144,** 2440–2452; doi:10.1016/j.jid.2024.03.040

INTRODUCTION

Pemphigus vulgaris (PV) is a potentially life-threatening autoimmune blistering skin disease (Kasperkiewicz et al, 2017; Schmidt et al, 2019). Autoantibodies (PV-IgG) against the desmosomal cadherins desmoglein (DSG)1 and DSG3 are the primary pathogenic antibodies, but antibodies against desmocollin 3 and other keratinocyte (KC) antigens appear to contribute to skin blistering as well (Amber et al, 2018; Egu et al, 2022a; Hudemann et al, 2022). The mechanisms involved include direct inhibition of DSG interaction and a complex, autoantibody- and epitope-specific signaling response that impairs KC adhesion by interfering with different steps of desmosome turnover (Spindler et al, 2018; Kitajima, 2014; Schmitt and Waschke, 2021; Schmitt et al, 2023). This is reflected by alterations of the desmosome ultrastructure in lesions from patients with PV, which are mimicked in human *ex vivo* skin models (Sokol et al, 2015; Egu et al, 2022a).

During the last decades, therapy for PV has improved dramatically by paradigms to deplete autoreactive B cells using the anti-CD20 mAb rituximab (Joly et al, 2007; Werth et al, 2021). Currently, the FcRn antagonist efgartigimod, which reduces the IgG autoantibody half-life, is trialed in a phase III study (Goebeler et al, 2022). However, especially for the acute phase of PV, additional therapeutics are required to reduce the amount of corticosteroids administered

[1]*Institute of Anatomy, Faculty of Medicine, Ludwig Maximilian University of Munich, Munich, Germany;* [2]*Lübeck Institute of Experimental Dermatology, University of Lübeck, Lübeck, Germany;* [3]*Department of Dermatology, University of Lübeck, Lübeck, Germany;* [4]*Faculty of Medicine and Health Sciences, University of Barcelona, Barcelona, Spain;* [5]*Department of Biomedicine, University of Basel, Basel, Switzerland; and* [6]*Institute of Anatomy and Experimental Morphology, University Medical Center Hamburg-Eppendorf, Hamburg, Germany*

[7]*These authors contributed equally to this work.*

[8]*These authors contributed equally to this work.*

Correspondence: Jens Waschke, Institute of Anatomy, Faculty of Medicine, Ludwig Maximilian University of Munich, Pettenkoferstrasse 11, D80336, Munich, Germany. E-mail: Jens.Waschke@med.uni-muenchen.de

Abbreviations: AFM, atomic force microscopy; DSG, desmoglein; ERK, extracellular signal–regulated kinase; KC, keratinocyte; NHEK, normal human epidermal keratinocyte; PF, pemphigus foliaceus; PTK, protein tyrosine kinase; PV, pemphigus vulgaris; STED, stimulated emission depletion microscopy; TEM, transmission electron microscopy

Received 6 October 2023; revised 23 March 2024; accepted 25 March 2024; accepted manuscript published online 19 April 2024; corrected proof published online 16 July 2024

because they have considerable side effects owing to high-dose usage (Yamagami et al, 2023). This notion has also recently been made by an independent expert panel (Ujiie et al, 2022). Recently, a first approach to stabilize KC adhesion was proposed in which the phosphodiesterase 4 inhibitor apremilast was demonstrated to reduce PV-IgG–induced skin blistering in human skin *ex vivo* and in a passive transfer mouse model *in vivo* (Sigmund et al, 2023). This strategy was based on the observation that cAMP is a central regulator of cadherin-mediated adhesion in different cell types (Vielmuth et al, 2023) and that cAMP-mediated phosphorylation of the desmosomal plaque protein plakoglobin at S665 is also involved in stabilization of cell adhesion in cardiomyocytes (Schinner et al, 2017). Because it is so far unclear whether patients with PV will benefit from these approaches, more treatment options are required to fulfill this unmet medical need. In addition, in preclinical pemphigus models, inhibition of other signaling pathways, namely, MAPK/extracellular signal–regulated kinase (ERK) kinase 1, TRKA, phosphoinositide 3-kinase alpha, and vascular endothelial growth factor, impaired the blister-inducing pathogenic activity of antibodies targeting DSG1 and DSG3 (Burmester et al, 2020). EGFR activation triggered by PV-IgG was shown to be involved in activation of signaling cascades leading to acantholysis (Frusić-Zlotkin et al, 2006). Pharmacological suppression of EGFR activity using erlotinib was protective in cultured KCs (Bektas et al, 2013; Walter et al, 2019) and mouse models (Sayar et al, 2014). In this study, we provide evidence that EGFR inhibition through erlotinib is effective to reduce PV-IgG–induced acantholysis in human skin and to rescue the desmosome ultrastructure by affecting DSG3 molecular-binding properties and propose that erlotinib can be repurposed to treat pemphigus.

RESULTS

EGFR inhibition prevents PV-IgG–induced loss of cell adhesion and enhances DSG3 molecular-binding properties

To investigate the involvement of EGFR in pemphigus in human skin, we analyzed lysates from human epidermis treated *ex vivo* with PV-IgG for 1 hour. Western blot analyses revealed significant PV-IgG–induced phosphorylation of EGFR at the Rous sarcoma-related kinase (SRC)-specific phosphorylation site Y845 and SRC phosphorylation at Y416. EGFR inhibition using erlotinib reduced EGFR but not SRC activation, indicating SRC to be upstream of EGFR (Figure 1a–c). Because inhibition of the receptor tyrosine kinase TRKA was shown to be protective against PV-IgG–induced acantholysis (Burmester et al, 2020), we evaluated effects on TRKA. PV-IgG increased expression and phosphorylation of TRKA at Y490, the latter of which was reduced after erlotinib treatment (Figure 1d and e).

To determine whether other kinases associated with EGFR signaling were modulated by pemphigus autoantibodies, we analyzed the kinome of protein tyrosine kinases (PTKs) regulated after treatment for 5, 30, or 120 minutes with PV-IgG, pemphigus foliaceus (PF) IgG, or control IgG of healthy human volunteers in human KCs (HaCaT) (Figures 1f–h). In line with the western blot results, PV-IgG activated several SRC family kinases (BLK, YES, FYN, FRK, LCK, and SRC, marked in green) but also kinases activating signaling pathways previously implicated in pemphigus pathogenesis such as RAS/ERK1/2, phosphoinositide 3-kinase/protein kinase B, and phospholipase Cγ/protein kinase C (marked in blue in Figure 1f). The latter kinases comprise RON; LYN; SYK; MET; and TRKA, TRKB, and TRKC, which all link EGFR signaling to the pathogenic pathways proposed before in pemphigus. Moreover, PV-IgG activated PTKs connecting SRC signaling to EGFR such as DDR1 and ABL (marked in red). STRING interaction modules depict strong connections between SRC family kinases and ABL and SRC as a connection node to pathways shown to be activated in PV (Figure 1h). In contrast, PF-IgG treatment did not cause activation of PTKs but rather induced significant inactivation of kinases, including JAK or ephrin-type receptors (Figure 1g and Supplementary Figure S1a).

To assess the effect of EGFR and ERBB2 inhibition, we performed dispase-based dissociation assays. Inhibition of EGFR alone with erlotinib or of both with lapatinib in normal human epidermal KC (NHEK) cells significantly reduced the number of fragments, restoring adhesion comparable with that in control conditions (Figure 1i and Supplementary Figure S1b). Next, we knocked down TRKA (Figure 1j), which was activated by PV-IgG in *ex vivo* skin as well as in the kinome analysis. TRKA knockdown restored adhesion in the dissociation assay comparable with that in control conditions (Figure 1k). Furthermore, we investigated the impact of TRKA on the ultrastructure of desmosomal components and keratin association in HaCaTs using stimulated emission depletion microscopy (STED). PV-IgG induced a fragmented staining of DSG3 with increased staining intensity and a retraction of keratin filaments from cell borders (Figure 2a–c). Knockdown of TRKA abolished keratin retraction but not fragmentation of DSG3 staining. Moreover, we used atomic force microscopy (AFM) to investigate the role of EGFR on DSG3-binding properties on living KCs. Treatment with erlotinib showed no alterations on the topography of NHEKs (Figure 2d). For measurements at cell borders, erlotinib led to a significant increase in the binding probability compared with the controls. This increase was restricted to cell borders and not visible at the cell surfaces. Subsequently, we analyzed the contribution of erlotinib for the binding strength, which was significantly increased at both cell borders and cell surfaces compared with that of controls. Finally, we analyzed the unbinding position of DSG3 interactions, which did not yield significant differences for all conditions.

To analyze the effect of erlotinib on DSG3 mobility in the cell membrane, fluorescence recovery after photobleaching experiments were conducted in NHEKs. Interestingly, erlotinib did not affect the overall availability of DSG3 in the cell membrane because there was no difference in the immobile fraction of DSG3 molecules compared with control conditions. However, a significantly increased recovery half time (Tau) has been observed, which suggests a slower movement of DSG3 within the cell membrane (Figure 2e). Rho-GTPase ELISA activation assays revealed that global activities of RhoA and RAC1 were not affected by erlotinib treatment in NHEK cells (Supplementary Figure S1c).

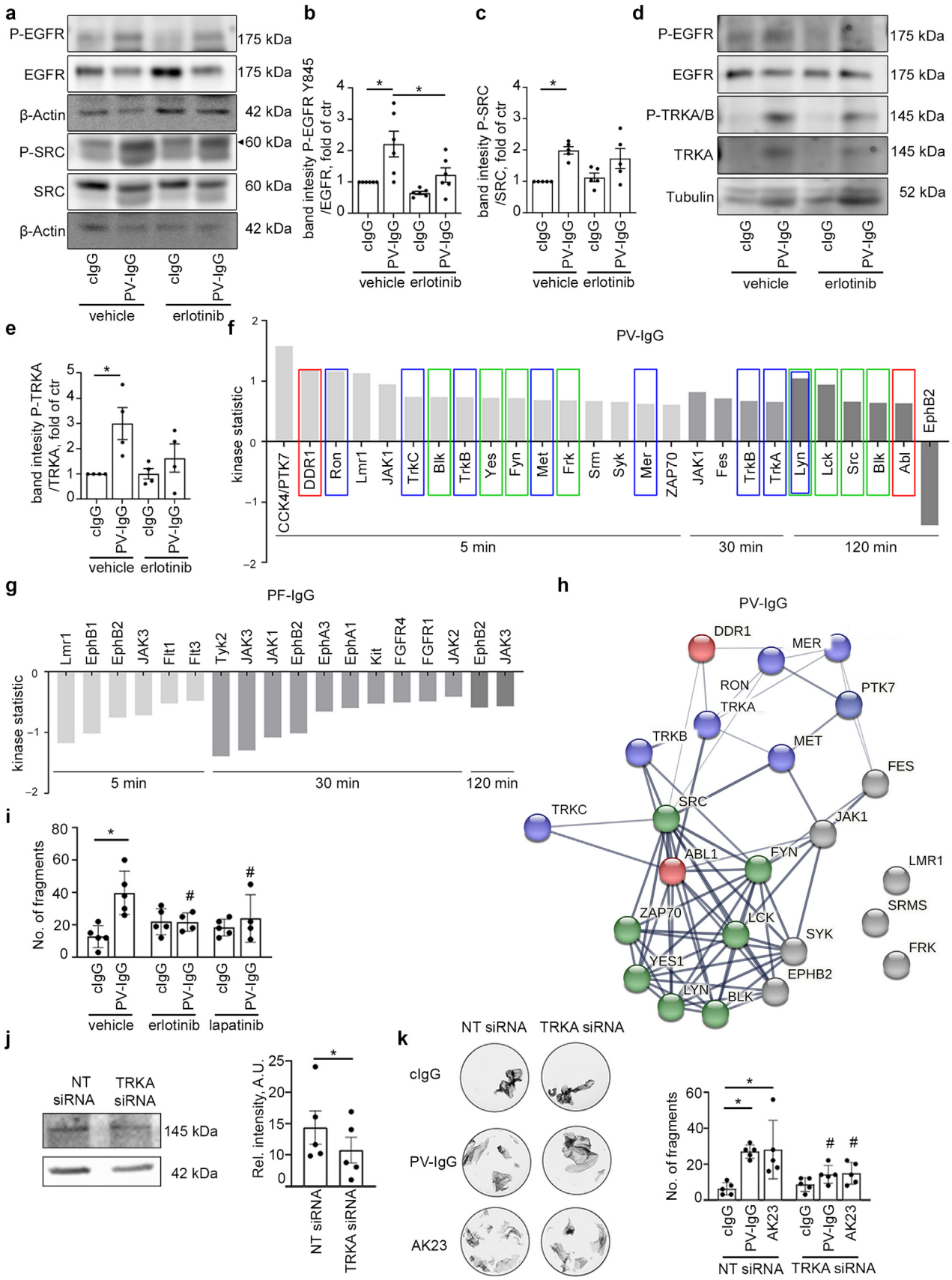

Figure 1. PV-IgG activates EGFR downstream targets, and EGFR inhibition prevented PV-IgG–induced loss of adhesion. (**a**–**e**) Western blot analysis of PV-IgG + erlotinib–treated human skin (n = 4–6). (**f**–**h**) Multiplex kinase profiling in PV-IgG/PF-IgG–treated HaCaT cells. Graphs show up/downregulation. STRING interactions at medium confidence level show predicted interactions (line thickness correlates with interaction strength) (green = SRC family, blue = kinases activating known pemphigus signaling pathways, red = kinases linking EGFR to SRC signaling, other colors are random; n = 3). (**i**) Dissociation assay in

EGFR inhibition abrogates PV-IgG–induced loss of desmosomes and major alterations in desmosome structure and keratin filament organization

We used STED imaging to investigate the pathomechanisms by which EGFR contributes to loss of cell adhesion in response to PV-IgG in NHEKs. We co-stained DSG1 and desmoplakin to determine changes in desmosome ultrastructure (Figure 3a–d). DSG1 was mostly located inside of desmosomes, however, extradesmosomal DSG1 was also present (Figure 3c). PV-IgG–induced fragmentation of DSG1 staining at cell borders was blocked by EGFR inhibition, which was paralleled by enhanced DSG1 staining intensity (Figure 3a and b). In addition, PV-IgG significantly reduced desmosome length and induced desmosomal widening in an EGFR-dependent manner (Figure 3d). In contrast, thickness of the desmoplakin plaque, a measure for plaque disorganization, was increased by PV-IgG treatment but not rescued by erlotinib.

Further STED analysis revealed a PV-IgG–induced fragmentation of DSG3 staining along cell borders as well as retraction and reduction of keratin filament insertion into DSG3-mediated contacts, all of which were rescued by erlotinib (Supplementary Figure S2a-c). EGFR inhibition decreased DSG3 fragmentation and was effective to increase the intensity of DSG3 staining under baseline conditions.

Erlotinib protects against PV-IgG–induced blister formation and alterations of desmosome ultrastructure in human skin *ex vivo*

In the human *ex vivo* pemphigus model (Egu et al, 2017), suprabasal blisters were detected in samples incubated with PV-IgG only but were significantly reduced in those also treated with erlotinib as confirmed by blister score analysis (Figure 4a and b). We also performed immunostaining for DSG1 and DSG3 showing fragmented staining after PV-IgG incubation, which was ameliorated by erlotinib (Supplementary Figure S3).

Next, we performed ultrastructural analysis of desmosomes in *ex vivo* skin samples using transmission electron microscopy (TEM) (Figure 4c). Desmosomes were smaller or split and sometimes absent at blister sites in samples injected with PV-IgG comparable with those in the skin lesions of patients with PV (Sokol et al, 2015). These hallmarks were ameliorated significantly by erlotinib (Figure 4c–f). Similarly, keratin filaments were retracted from the cell borders to the perinuclear region, and plaque organization was aberrant in PV-IgG–treated skin samples, both of which were rescued by EGFR inhibition (Figure 4g and h). Finally, we scrutinized the presence of desmosome midlines, which are characteristic of mature hyperadhesive epidermal cells (Garrod and Kimura, 2008). Desmosome midlines were drastically reduced in PV-IgG–injected samples but were rescued by EGFR inhibition (Figure 5a and b).

In comparison with TEM, intact human *ex vivo* epidermis was co-stained for DSG3 and keratin filaments and evaluated by STED microscopy (Figure 5c). PV-IgG–induced blister formation was paralleled by fragmented DSG3 staining along cell borders, with few high staining intensity clusters remaining (Figure 5d). In erlotinib-treated samples, we evaluated sites where blister formation was not completely prevented. Both, the fragmentation of DSG3 staining and keratin retraction at the basal–suprabasal interface of perilesional cells were significantly reduced, similar to those in the control conditions (Figure 5d and e). In summary, the results reflect the findings revealed by TEM in intact epidermis as well as by STED microscopy in NHEK cells *in vitro*.

DISCUSSION

New therapeutic paradigms for treatment of pemphigus patients during the acute-phase would fulfill an unmet medical need. They are required to reduce corticosteroid dosage during the first weeks of autoantibody-reducing strategies such as rituximab. In this study, we provide evidence that EGFR inhibition by erlotinib, which, similar to other related molecules, is used for treatment of cancer (Sabbah et al, 2020; Sridhar et al, 2003), is effective to reduce PV-IgG–induced epidermal blistering in human skin, and thus may be repurposed for treatment of pemphigus. In human epidermis, we demonstrated that EGFR is activated downstream of SRC, and identified TRKA to be involved in EGFR signaling. Mechanistically, PV-IgG was found to activate a robust kinase response associated with EGFR signaling, including different SRC family kinases but also molecules linking EGFR to downstream pathways associated with loss of cell adhesion and skin blistering in pemphigus (Burmester et al, 2020; Kaur et al, 2022; Schmitt and Waschke, 2021). EGFR inhibition rescued desmosome ultrastructure from PV-IgG–induced alterations and, at molecular level, increased DSG3-binding frequency and force as well as cytoskeletal anchorage.

Role of EGFR signaling in pemphigus acantholysis and associated mechanisms

There is ample evidence for the involvement of EGFR in PV-IgG–induced loss of KC adhesion leading to acantholysis. First, it was demonstrated that EGFR activation induced plakoglobin phosphorylation and desmosome disassembly leading to loss of cell adhesion (Gaudry et al, 2001; Yin et al, 2005). Afterward, PV-IgG was shown to induce intercellular gap formation in cultured KCs, which was prevented by EGFR inhibition (Bektas et al, 2013). Furthermore, PV-IgG activated ERK1/2, downstream of EGFR (Frusić-Zlotkin et al, 2006). EGFR was shown to be phosphorylated at Y845, indicative of SRC-mediated EGFR transactivation in response to PV-IgG and AK23 *in vitro* after 30–120 minutes (Bektas et al, 2013; Chernyavsky et al, 2007; Schulze et al, 2012; Walter et al, 2019) and 24 hours of AK23 incubation also at Y1173, which is in line with canonical activation by EGF and related ligands upregulated in ADAM10-dependent manner after PV-IgG binding (Ivars et al, 2020; Kugelmann et al,

PV-IgG + erlotinib/lapatinib–treated NHEK cells (n = 4–5). (**j**) Western blot and (**k**) dissociation assay of HaCaTs after KD of TRKA. Cells were treated with PV-IgG or AK23 (n = 4–5). * denotes significant as indicated, and # denotes significant to corresponding control. Two-way ANOVA with Sidak's (for **i** and **k**) or Bonferroni (for **a**) correction or *t*-test (for **j**) was used. $P \leq 0.05$. cIgG, control IgG; KD, knockdown; min, minute; NHEK, normal human epidermal keratinocyte; P-EGFR, phosphorylated EGFR; PF, pemphigus foliaceus; P-SRC, phosphorylated SRC; P-TRKA, phosphorylated TRKA; PV, pemphigus vulgaris.

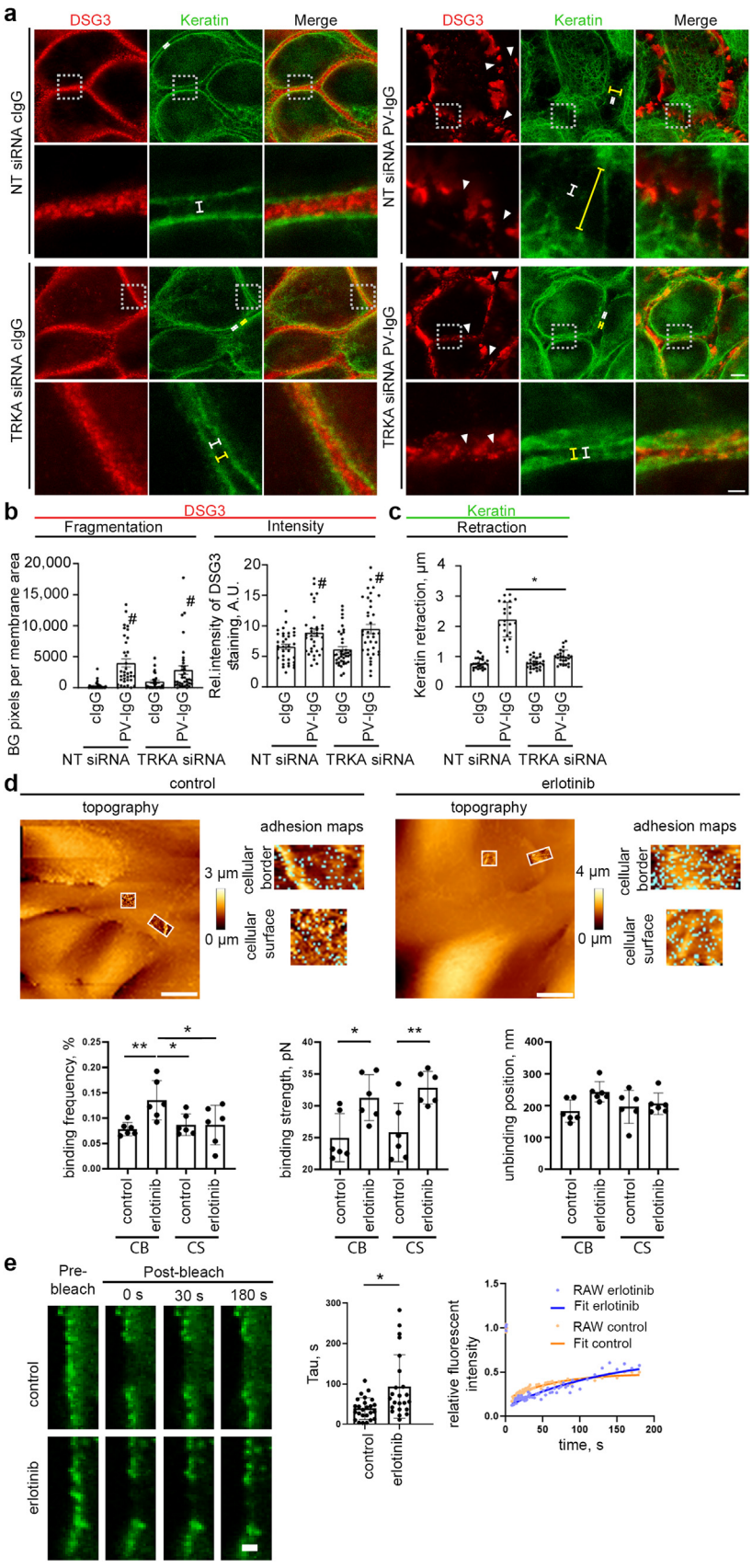

Figure 2. PV IgG–induced ultrastructural reorganizations are TRKA dependent and EGFR inhibition enhanced DSG3-binding properties. (**a**) STED images of costaining of DSG3 (red) and pan-cytokeratin (green) after TRKA KD and PV-IgG treatment. Spans: keratin distance (yellow), control (white). Bars = 2 µm (overview) and 0.5 µm (zoom). Arrowheads: Fragmented staining. Quantification of (**b**) DSG3 and (**c**) keratin staining (n = 6). (**d**) AFM topography and DSG3 adhesion maps. Cyan dots: Median DSG3 interactions (n = 3). Bars = 5 µm. Adhesion maps at CBs consist of 800 force–distance curves and 625 force–distance curves at CS. (**e**) Bleached cell borders from FRAP measurements (left) (bar = 2 µm), recovery half time (TAU) (middle), and fluorescent intensity recovery curve (right) (n = 3). $^{*}P \leq 0.05$ and $^{**}P \leq 0.01$ represent statistical significance in Two-way ANOVA followed by Sidak's (for **b** and **c**), Tukey's (for **d**) multiple comparison test or *t*-test (for **e**). All experiments were performed in HaCaTs. AFM, atomic force microscopy; CB, cell border; CS, cell surface; DSG, desmoglein; FRAP, fluorescence recovery after photobleaching; KD, knockdown; PV, pemphigus vulgaris; siRNA, small interfering RNA; STED, stimulated emission depletion microscopy.

2022; Pretel et al, 2009; Schulze et al, 2012). In line with this, EGFR inhibition using erlotinib significantly reduced PV-IgG– but not PF-IgG–mediated loss of cell adhesion *in vitro*, supporting that EGFR activation may be caused by autoantibodies against DSG3 (Walter et al, 2019). In agreement with this, EGFR phosphorylation at Y845 was shown recently in

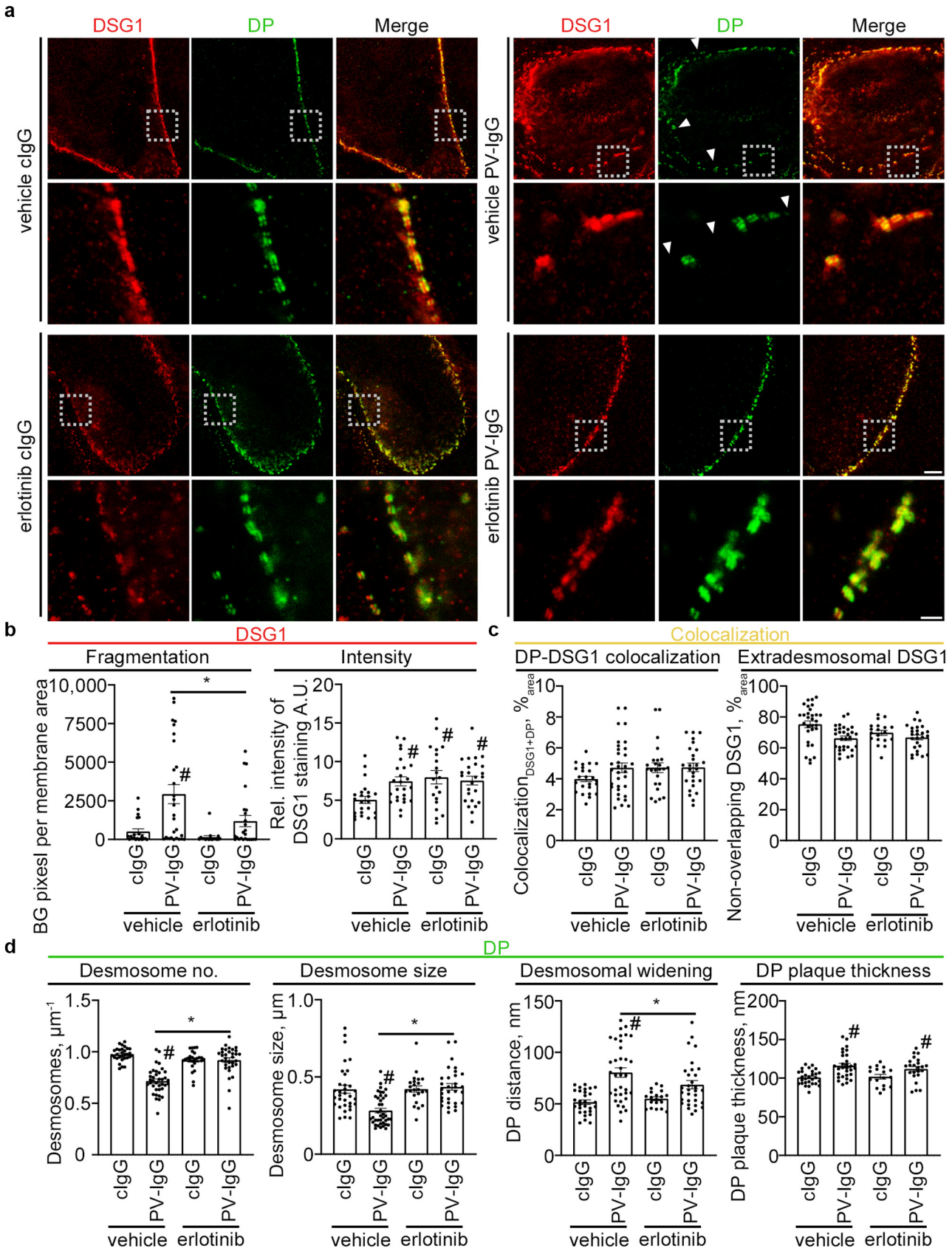

Figure 3. STED microscopy revealed the protective mechanisms of EGFR inhibition in keratinocytes. (**a**) Co-staining of DSG1 (red) and DP (green) in NHEK cells treated with PV-IgG and erlotinib. Arrowheads: Regions lacking desmosomes. Bars = 2 µm (overview) and 0.5 µm (zoom). (**b**) Quantification of DSG1 staining. (**c**) Quantification of colocalization of membranous DSG1 and DP. (**d**) Quantification of DP (n = 4–8). * denotes statistically significant differences as

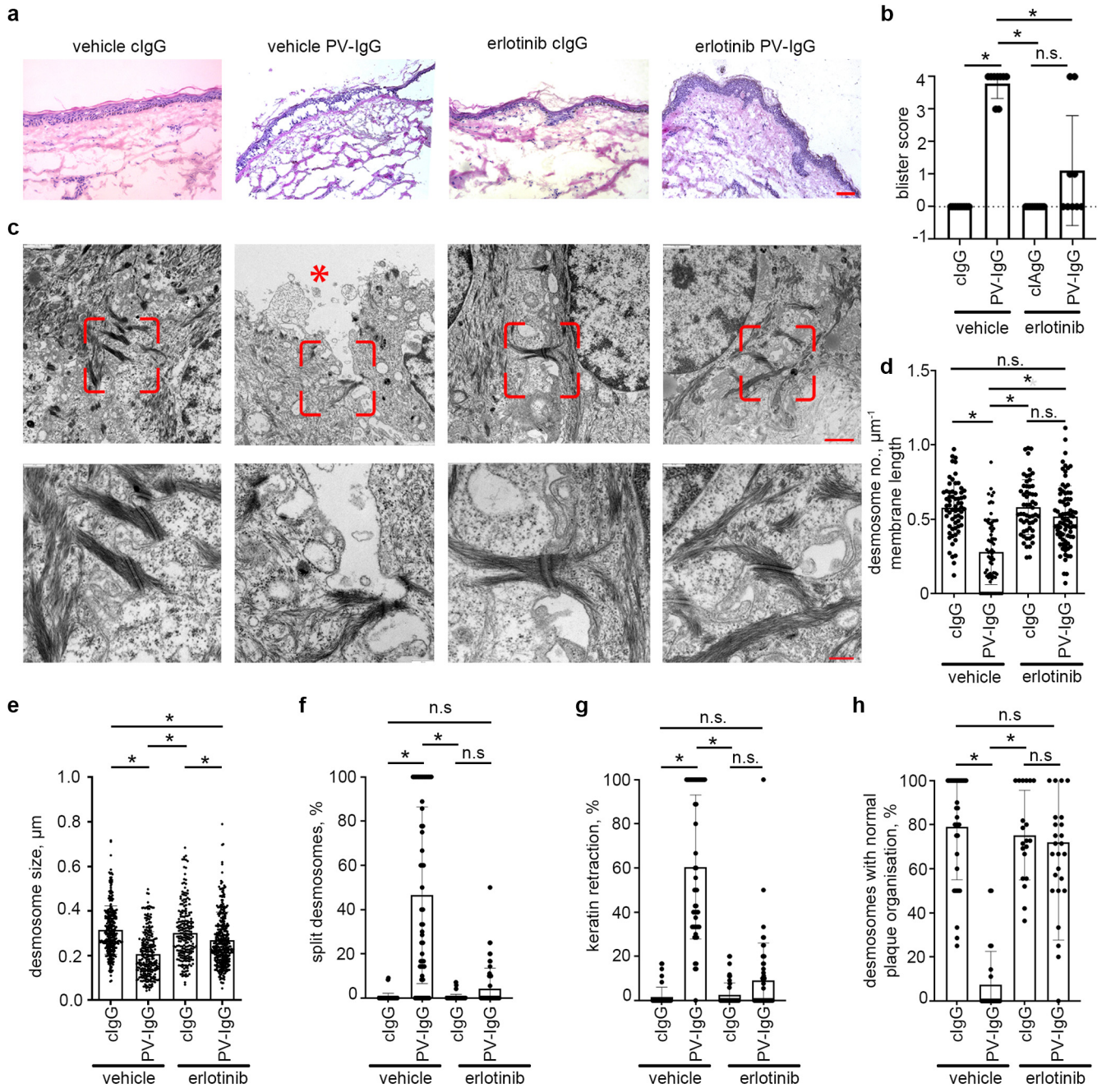

Figure 4. Protective effect of erlotinib against blistering and alterations of desmosome ultrastructure in human skin. (**a**) H&E staining of human skin samples incubated with PVIgG showing blister formation averted by erlotinib. Bar = 100 µm. (**b**) Blister score showing a significant reduction of suprabasal cleft formation after erlotinib addition (n = 8). (**c**) TEM micrographs showing altered desmosome ultrastructure in PV-IgG–injected samples, which was ameliorated by preincubation with erlotinib. Bars = 1 µm (overview) and 250 nm (zoom). * indicates blister regions. Ultrastructural quantification of (**d**) desmosome number, (**e**) size, (**f**) percentage split desmosomes, (**g**) percentage keratin retraction, and (**h**) percentage desmosomes with normal plaque organizations (n = 3–4). * denotes statistically significant differences. Two-way ANOVA with Sidak's posthoc analysis was conducted. $P \leq 0.05$. cIgG, control IgG; DP, desmoplakin; PV, pemphigus vulgaris; TEM, transmission electron microscopy.

murine hair follicles after incubation with AK23 (Hariton et al, 2023). Besides, different inhibitors of EGFR signaling, including erlotinib, lapatinib, CL387785, and the EGFR-blocking antibody cetuximab, protected against AK23- and PV-IgG–induced skin blistering in mice (Ivars et al, 2020; Pretel et al, 2009; Sayar et al, 2014). Interestingly, when PV-IgG contained autoantibodies against desmocollin 3, this protective effect was lost, which is in line with the observation that pathogenic anti–desmocollin 3 autoantibodies from mice did not activate EGFR (Hudemann et al, 2022; Ivars

indicated, and # denotes the corresponding control condition. Two-way ANOVA with Sidak's posthoc analysis was conducted. $P \leq 0.05$. DP, desmoplakin; DSG, desmoglein; NHEK, normal human epidermal keratinocyte; PV, pemphigus vulgaris; STED, stimulated emission depletion microscopy.

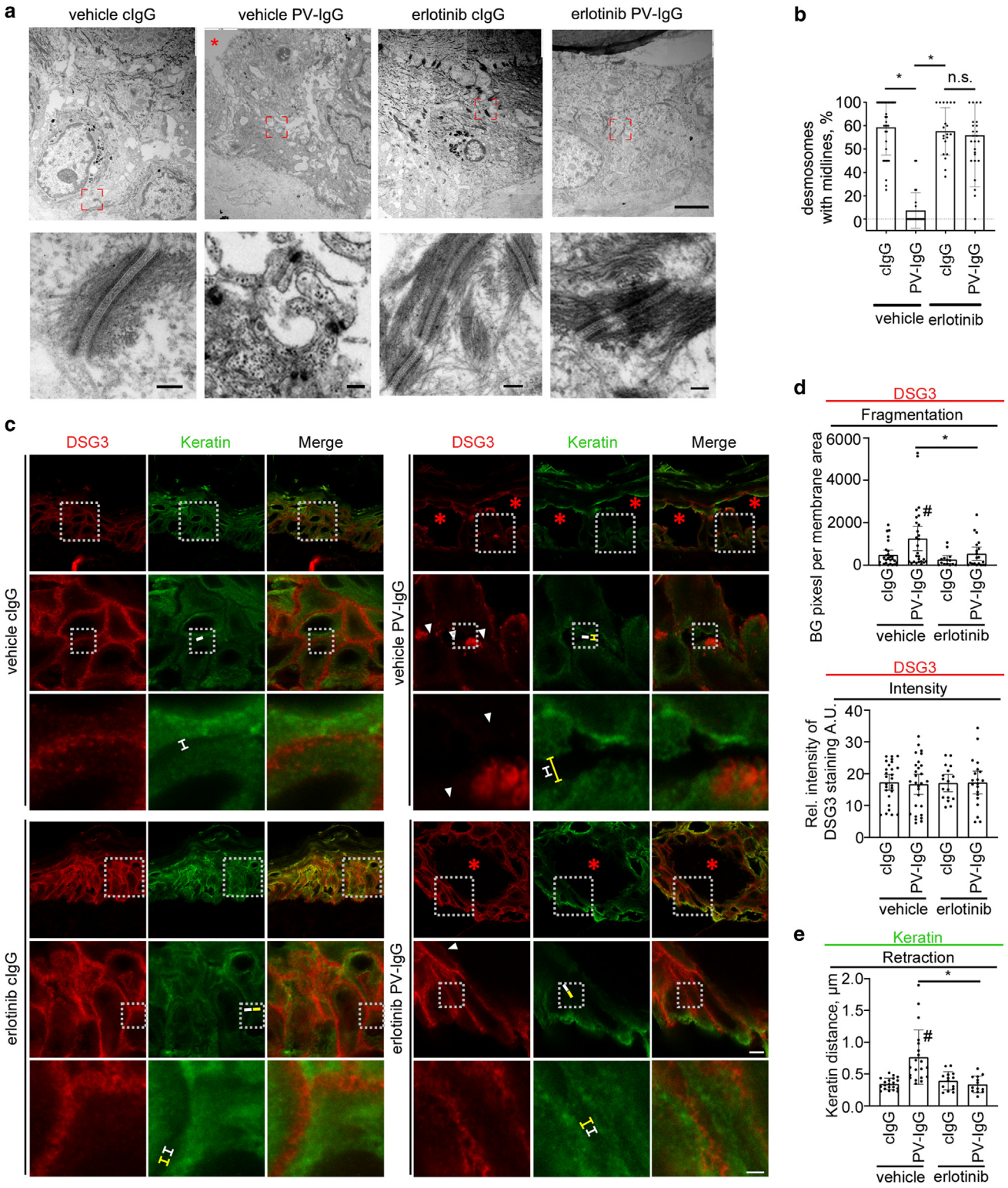

Figure 5. EGFR inhibition rescued desmosome midlines and other ultrastructural features in human skin *ex vivo*. (**a**) Electron micrograph panorama showing basal and immediate suprabasal epidermal layers (upper panel), zoomed to desmosome midlines (lower panel). Bars = 2.5 µm and 100 nm, respectively. (**b**) Quantification of the relative occurrence of desmosome midlines (n = 3). (**c**) STED microscopy images of a co-staining of DSG3 (red) and pan-cytokeratin (green) in human skin *ex vivo* injected with PV-IgG and erlotinib. Spans: Keratin filament distance (yellow), control (white). Arrowheads: fragmented staining of DSG3. Bars = 2 µm (overview) and 0.5 µm (zoom). (**d**) Quantification of DSG3 staining and (**e**) keratin filament retraction (n = 4–8). * indicates blister regions, * indicates statistically significant differences as indicated, and # denotes the corresponding control condition, in Two-way ANOVA with Sidak's posthoc analysis for multiple comparisons $P \leq 0.05$. cIgG, control IgG; DSG, desmoglein; n.s., not significant; PV, pemphigus vulgaris; STED, stimulated emission depletion microscopy.

et al, 2020). Taken together, these results indicate that EGFR is involved primarily in skin blistering induced by autoantibodies targeting DSG3 but not desmocollin 3 and may explain why some PV-IgG fractions induced pathogenic effects independent of EGFR (Heupel et al, 2009). In this scenario, rapid EGFR activation appears to be mediated by SRC-induced transactivation in a p38MAPK-dependent manner (Bektas et al, 2013; Schmitt et al, 2023).

However, SRC inhibition was found to be protective against PV-IgG– and AK23-induced blistering in mice but not in human skin (Ivars et al, 2020; Kugelmann et al, 2019; Pretel et al, 2009). This raised the possibility that EGFR inhibition also would be protective only in mice, where DSG3 is much more critical for epidermal integrity than in humans. This can be concluded from the sufficiency of DSG3-specific antibodies such as AK23 and 2G4 to cause skin blistering in the murine passive transfer model but not in the human *ex vivo* skin model (Egu et al, 2017; Hofrichter et al, 2018; Hudemann et al, 2022; Spindler et al, 2013a). Thus, the human *ex vivo* model reflects the situation in patients more accurately than the murine passive transfer model because patients suffer from mucosal PV under these conditions but show no skin involvement (Schmidt et al, 2019).

This study demonstrates that EGFR inhibition through erlotinib is effective to prevent blistering in human skin and provides insights into the mechanisms involved. We detected activation of EGFR and SRC in human skin upon incubation with PV-IgG using the *ex vivo* skin model. Moreover, TRKA—the inhibition of which was shown to be protective in PV, and its crosstalk with EGFR was reported in monocytes—was also activated (Burmester et al, 2020; El Zein et al, 2010). These findings are strengthened by the kinome data indicating that TRKA and SRC family members were activated upon treatment with PV-IgG. Inhibition of EGFR by erlotinib prevented the phosphorylation of TRKA and EGFR but not of SRC, indicating SRC phosphorylation to be upstream and TRKA phosphorylation to be downstream of EGFR. This is in line with previous findings in which EGFR activation was shown to be SRC dependent in cultured KCs (Walter et al, 2019). The kinome data also show that PV-IgG but not PF-IgG triggered a robust tyrosine kinase response, which supports the hypothesis that signaling in pemphigus pathogenesis is autoantibody specific (Schmitt and Waschke, 2021) and that SRC-mediated EGFR activation is mediated by autoantibodies against DSG3 but not against DSG1 (Walter et al, 2019, 2017). Specifically, isoforms from all 3 SRC subfamilies were found to be activated over the time course of 120 minutes, similar to ABL, which is also related to EGFR signaling (Peschard and Park, 2003; Tanos and Pendergast, 2006; Fernow et al, 2009). Because the SRC family kinase inhibitor PP2 was not effective to prevent PV-IgG–induced acantholysis in human skin (Kugelmann et al, 2019), the significant effect of erlotinib may be attributed to the fact that EGFR regulates several other signaling pathways such as p38MAPK, MAPK/ERK/ERK1/2, phosphoinositide 3-kinase/protein kinase B, and phospholipase Cγ/protein kinase C. This is intriguing because all these signaling pathways are associated with loss of cell adhesion and skin blistering in pemphigus (Schmitt and Waschke, 2021). The phosphotyrosine kinome also identified several molecules by which PV-IgG can activate these pathways, including RON; LYN; SYK; MET; and TRKA, TRKB, and TRKC (Avila et al, 2012; Danilkovitch-Miagkova, 2003; Gupta et al, 2022; Iqbal et al, 2010; Law et al, 1996; Takano et al, 2002; Trusolino et al, 2010) as well as molecules linking EGFR to SRC signaling such as DDR1 and ABL (Fernow et al, 2009; Matada et al, 2021; Tanos and Pendergast, 2006). Among these, TRK members are especially interesting because inhibitors of TRKA, similar to small molecules targeting phosphoinositide 3-kinase and MAPK/ERK kinase 1, have been recently identified to be protective against PV-IgG–induced acantholysis (Burmester et al, 2020), indicating that these pathways are indeed relevant for pemphigus pathogenesis.

Therefore, we knocked down TRKA to examine the mechanism by which PV-IgG triggered EGFR signaling. TRKA knockdown preserved cell adhesion and keratin anchorage after PV-IgG treatment comparable with EGFR inhibition. In contrast, fragmentation of DSG3 staining was not ameliorated by TRKA depletion but only after EGFR inhibition. These results suggest that TRKA is one of several downstream targets of EGFR as indicated by the kinome analysis and are consistent with previous findings that showed TRKA inhibition was protective against alterations of DSG3 staining induced by 1 of 2 PV-IgG fractions only (Burmester et al, 2020).

It has been demonstrated that biopsies from patients with PV reveal ultrastructural alterations, which are hallmarks for the disease and can be explained only by complex mechanisms interfering with desmosome turnover (Kitajima, 2014; Sokol et al, 2015). The *ex vivo* human skin model closely reflects these alterations, which have been characterized in detail before (Egu et al, 2022a). In this study, we demonstrate by TEM that loss of desmosomes as well as reduction of desmosome size, formation of split desmosomes, and keratin filament retraction are abolished by erlotinib. Moreover, we also analyzed the presence of desmosome midlines within the extracellular space, which is regarded as a measure of mature, hyper-adhesive desmosomes and is thus the most sensitive ultrastructural correlate for desmosome integrity (Garrod et al, 2005). We found that PV-IgG reduced the number of desmosomes with midlines, which was blocked by erlotinib. Moreover, STED imaging in KCs supported the findings from the *ex vivo* model, indicating that *in vitro* experiments can be used to study the mechanisms underlying PV-IgG–induced loss of KC adhesion. In this study, fragmentation of DSG1, DSG3 immunostaining, and other structural hallmarks of PV were observed, in addition to the parameters revealed by TEM, which supports a previous study using confocal imaging (Bektas et al, 2013). Interestingly, erlotinib alone enhanced DSG3 staining intensity, which is in line with AFM experiments showing that DSG3-binding frequency was enhanced, indicating an increased amount of DSG3 available at cell borders. In addition, single-molecule binding strength of DSG3 was enhanced as well. Finally, the prolonged recovery half time after erlotinib treatment can be taken as a measure of cytoskeletal anchorage (Sigmund et al, 2023) and is comparable with the effects of erlotinib-mediated inhibition of keratin filament reorganization described earlier.

Taken together, these data indicate that EGFR signaling regulates the molecular binding properties of DSG3, and

erlotinib is effective to abolish autoantibody-induced alterations of desmosome ultrastructure. The protective effects of erlotinib, including strengthening of cell adhesion, were comparable with findings in a model for arrhythmogenic cardiomyopathy, which also is a desmosome disease (Shoykhet et al, 2023). This suggests that at least some mechanisms regulating desmosome adhesion are conserved among different tissues (Spindler et al, 2023).

Erlotinib to stabilize desmosomal adhesion as a treatment paradigm in pemphigus

We propose that erlotinib can be used to treat patients with pemphigus because it is approved for doses comparable with those in our study (https://www.ema.europa.eu/en/documents/product-information/tarceva-epar-product-information_en.pdf). Erlotinib is effective to stabilize KC adhesion, similar to the phosphodiesterase 4 inhibitor apremilast (Sigmund et al, 2023), but may be suitable for different patients dependent on the side effect profile. Because EGFR inhibition rescued all ultrastructural parameters of desmosomes and abrogated depletion of DSG1 and DSG3, whereas apremilast preserved keratin filament organization only, erlotinib may even be more effective. Further studies in patients are required to delineate the efficacy of both mediators as additional treatment paradigms in pemphigus.

MATERIALS AND METHODS

For a detailed description, please refer to Supplementary Materials. Mediators, antibodies, companies, materials, and software can be found in Supplementary Tables S1 to S5

PamGene measurement

For PTK profiling, HaCaTs were treated with IgGs for indicated time points, lysed using M-PER-buffer, and centrifuged (15 minutes; 4 °C; 19,000*g*).

Multiplex kinase activation profiling was performed with the supernatants using the PamChip PTK peptide microarray system from PamGene International B.V. according to the manufacturer's instructions. Detection of substrate phosphorylation signals through emitted fluorescence was enabled by a computer-controlled charge-coupled device camera and measured repeatedly using Evolve software during a 1-hour kinetic protocol. Resulting images were analyzed using the BioNavigator Software, with the predesigned protocol PTK Image Analysis and evaluated with PTK Basic Processing. A kinase was considered to be regulated if the mean specificity score was ≥ 1 ($P \leq 0.1$) and the significance score was ≥ 0.4 ($P \leq 0.32$) (Zillikens et al, 2021). Pemphigus IgG samples were compared with the control IgG samples for the same time points. The pathway ontology was performed using the STRING database (Jensen et al, 2009).

Cell culture

Primary NHEKs in passages 2−6 were cultivated in CnT-Prime Basal Medium 1 at low calcium (0.06 mM) until confluency and switched to 1.8 mM calcium for differentiation for 24 hours. The human KC cell line (HaCaT) was cultured in DMEM with 10% fetal calf serum, 50 U/ml penicillin, and 50 g/ml streptomycin both at 37 °C in a humidified atmosphere of 5% carbon dioxide.

Incubation

Cells were preincubated with the mediators for 1 hour before IgG treatment. For Rho-GTPase ELISA, the mediators were added 2 hours before cell lysis. For concentration of mediators, refer to Supplementary Table S1. Knockdown was performed with 100 nmol/ml of small interfering RNA and transfected using Lipofectamine RNAiMAX Reagent for 24 hours in accordance with the corresponding supplier instructions.

SDS cell and *ex vivo* skin lysis

Cells cultured in 12-well plates or *ex vivo* skin samples were lysed using SDS lysis buffer containing phosphatase and protease inhibitors. Tissues were homogenized using gentleMACS Tissue Dissociator and centrifugated at 7000 *g* for 1.5 minutes. The protein amount was determined with a Pierce BCA protein assay kit. For western blotting, 20 µg of cell lysates and 40 µg of skin lysates were used.

Western blot analysis

Electrophoresis and western blotting were performed using standard protocols. Primary antibodies were added overnight at 4 °C in 5% BSA in Tris-buffered saline with Tween 20 and secondary antibodies for 1 hour (Supplementary Table S2).

Dispase-based dissociation assay

Confluent monolayers of NHEKs or HaCaTs were washed with Hanks Buffered Saline Solution incubated with 2.4 U/ml dispase II in Hanks' Balanced Salt Solution for 10 minutes at 37 °C and 95% humidity. After detachment of the monolayer, the reaction was stopped by adding 200 µl Hanks' Balanced Salt Solution. Shear stress was applied using an electrical pipette to produce a defined output, and fragment numbers were determined.

Rho-GTPase ELISA

The intracellular RAC1 and RhoA GTPase activity of NHEK cells was measured using a G-protein ELISA kit according to the company instructions.

Immunostaining for STED microscopy

NHEK cells or 6-µm *ex vivo* skin cryosections on high precision glass cover slips were fixed with ethanol/acetone and blocked with 3% BSA and 1% normal goat serum in PBS for 30 minutes. Primary antibodies were incubated for 3 hours, secondary antibodies for 1 hour, and DAPI for 15 minutes (Supplementary Table S2). The coverslips were mounted on glass slides using Prolong Diamond Antifade Mountant.

For imaging, an Abberior 3D STED confocal microscope with IMMOIL-F30CC was used. Star Red was excited at 638 nm and Alexa 594 at 594 nm using pulsed diode lasers. Fluorophore depletion was achieved with a pulsed fibre laser (PFL-P-30-775B1R, MPB Communications) at 775 nm.

AFM

AFM experiments were conducted as described before (Hiermaier et al, 2021). Briefly, a NanoWizard 3 AFM on an inverted optical microscope was used with MLCT cantilevers functionalized with recombinant DSG3-Fc protein. NHEK cells were probed to detect specific DSG3 single-molecule interactions and cell topography using existing protocols (Fuchs et al, 2022; Vielmuth et al, 2015). Topographic imaging was done using QI (setpoint: 0.5 nN, Z-length: 1500 nm, pulling speed: 30 µm/s) and force mapping mode for adhesion maps (setpoint: 0.5 nN, Z-length: 1500 nm, pulling speed: 10 µm/s, extend delay: 0.1 seconds). Adhesion maps were measured either across cell borders or on the apical cell surface.

Fluorescence recovery after photobleaching

Fluorescence recovery after photobleaching experiments were conducted as described earlier (Hiermaier et al, 2021). In brief, NHEKs were transfected with pEGFP-N1-DSG3, provided by Yasushi Hanakawa, using Lipofectamine 3000. Erlotinib incubation was conducted 1 hour prior to experiments. Imaging was performed at 37 °C with 5% carbon dioxide and constant humidity on a Leica SP5 inverted microscope. Data were analyzed with the fluorescence recovery after photobleaching wizard software provided by Leica.

Ex vivo skin pemphigus model

Human skin biopsies (~4 cm^2) were excised from healthy body donors from the body donor program (Institute of Anatomy and Cell Biology, Ludwig-Maximilians-Universität München, Munich, Germany) received maximal of 24 hours after decease as described before (Egu et al, 2017). Body donors provided written informed consent for use of samples for research purposes, and this has been approved by the local ethical committee of Ludwig-Maximilians-Universität München. Tissue viability was determined using MTT. A total of 50 µl of mediators and after 1 hour PV-IgG was intradermally injected, followed by floating incubation in HaCaT medium for 24 hours. Afterward, the samples were gently rubbed 6 times using a rubber head to apply mechanical stress to induce blister formation.

Purification of patients IgG fractions and AFM proteins

Sera from a healthy volunteer as well as from patients with mucocutaneous PV or PF were purified using protein A affinity chromatography as described before (Spindler et al, 2013b). Ethical approval was provided by the local ethical committee of University of Lübeck (number AZ12-178). Briefly, IgG fractions (Supplementary Table S3) were incubated with protein A agarose in purification columns for 2 hours, washed with PBS, eluted with 20 mmol/l sodium citrate, neutralized in 2 mol/l sodium carbonate solution, and concentrated in a filter unit at 19,000 *g* for 20 minutes.

The recombinant DSG3-Fc construct (full extracellular domain of DSG3) was purified as described previously (Heupel et al, 2008). Constructs were expressed in Chinese hamster ovarian cells and isolated from the supernatant by protein-A agarose affinity chromatography (described earlier).

Histology and immunostaining of skin sections

The skin tissue was processed for histology, and blister score was determined as described before (Egu et al, 2017). For immunostaining, sections were heated at 60 °C (30 minutes), fixed with 2% paraformaldehyde in PBS (10 minutes), permeabilized with 0.1% Triton X-100 (1 hour), and blocked with 3% BSA and 1% normal goat serum (1 hour). Primary antibodies (Supplementary Table S2) were incubated overnight at 4 °C. Secondary antibodies, Cy3-conjugated goat anti-mouse, and Cy2-conjugated goat anti-rabbit were applied for 1 hour at room temperature protected from light. DAPI was applied for 10 minutes to visualize the nuclei. Finally, slides were mounted with 1.5% n-propyl gallate in glycerol, and images were captured using a SP5 confocal microscope with an ×63 numerical aperture of 1.4 PL APO objective.

Electron microscopy

The skin samples were sliced into small pieces, ~2 mm^2, fixed in 2.5% glutaraldehyde in PBS at room temperature, and subsequently processed for electron microscopy as described previously (Egu et al, 2017). Images were captured at ×4000 and ×12,500 magnifications with a Libra 120 TEM equipped with a SSCCD camera system. ImageSP software was used for constructing panorama images.

Ultrastructural quantification

Electron micrographs of lateral and apical desmosomes of basal KCs were captured and considered for evaluation. Images taken at ×4000 magnification were used for quantification, and for each set of experiments, 15−20 images and ~100 desmosomes were evaluated for each condition. Desmosome profiles were defined, and different desmosome parameters were evaluated as previously described (Egu et al, 2022b).

Image processing and statistical analysis

Origin Pro 2016G was used for analyzing AFM data. Image processing was performed with Photoshop CS5 and LAS X life science. ImageJ was used to quantify fluorescence staining (immunofluorescence) and band intensity (western blot) and desmosome parameters (electron microscopy). AFM data were analyzed with JPK Data Processing software. For desmosome size in electron microscopy, each desmosome is represented by a single data point, whereas for other evaluations, each data point represents the average per electron micrograph or STED image. Comparison of datasets was performed using *t*-test or 2-way ANOVA with Sidak or Bonferroni posthoc test using Prism ($P < 0.05$). All data are presented as mean ± SEM.

DATA AVAILABILITY STATEMENT

The data underlying this article will be made available by the authors, without undue reservation, to any qualified researcher. No large dataset was generated.

ORCIDs

Desalegn Tadesse Egu: http://orcid.org/0000-0003-0145-0823
Thomas Schmitt: http://orcid.org/0000-0003-3781-7236
Nancy Ernst: http://orcid.org/0000-0002-3248-2425
Ralf Joachim Ludwig: http://orcid.org/0000-0002-1394-1737
Michael Fuchs: http://orcid.org/0000-0002-7816-3438
Matthias Hiermaier: http://orcid.org/0000-0001-6035-6517
Sina Moztarzadeh: http://orcid.org/0000-0001-7519-598X
Carla Sebastià Morón: http://orcid.org/0009-0003-5382-2219
Enno Schmidt: http://orcid.org/0000-0002-1206-8913
Vivien Beyersdorfer: http://orcid.org/0009-0001-2575-500X
Volker Spindler: http://orcid.org/0000-0002-1302-5421
Letyfee Sarah Steinert: http://orcid.org/0000-0002-3244-4613
Franziska Vielmuth: http://orcid.org/0000-0002-8570-7595
Anna Magdalena Sigmund: http://orcid.org/0000-0001-8533-9617
Jens Waschke: http://orcid.org/0000-0003-1182-5422

CONFLICT OF INTEREST

The authors state no conflict of interest.

ACKNOWLEDGMENTS

We thank Martina Hitzenbichler, Silke Gotschy, and Michelle Hermann for their excellent technical assistance as well as Jessica Plewa, Michael Becker, Manuela Kunz, and Axel Unverzagt for their assistance with body donor preparations. This work was supported by Deutsche Forschungsgemeinschaft FOR 2497 TP5 to JW.

AUTHOR CONTRIBUTIONS

Data curation: DTE, TS, AMS, MF, MH, LSS, CSM; Formal Analysis: DTE, TS, AMS; MF, MH; Funding Acquisition: JW; Investigation: DTE, TS, AMS, MF, MH, LSS, CSM, FV; Methodology: DTE, TS, AMS, MF, MH; Project Administration: DTE; Resources: VB, VS, TS, MF, MH, AMS; Supervision: JW; Validation: JW, DTE, TS, AMS; Visualization: JW, AMS, DTE, TS. Writing - Original Draft Preparation: DTE, TS, AMS, JW; Writing - Review and Editing: JW, AMS, DTE, TS

SUPPLEMENTARY MATERIAL

Supplementary material is linked to the online version of the paper at www.jidonline.org, and at https://doi.org/10.1016/j.jid.2024.03.040.

REFERENCES

Amber KT, Valdebran M, Grando SA. Non-desmoglein antibodies in patients with pemphigus vulgaris. Front Immunol 2018;9:1190.

Avila M, Martinez-Juarez A, Ibarra-Sanchez A, Gonzalez-Espinosa C. Lyn kinase controls TLR4-dependent IKK and MAPK activation modulating the activity of TRAF-6/TAK-1 protein complex in mast cells. Innate Immun 2012;18:648–60.

Bektas M, Jolly PS, Berkowitz P, Amagai M, Rubenstein DS. A pathophysiologic role for epidermal growth factor receptor in pemphigus acantholysis. J Biol Chem 2013;288:9447–56.

Burmester IAK, Flaswinkel S, Thies CS, Kasprick A, Kamaguchi M, Bumiller-Bini V, et al. Identification of novel therapeutic targets for blocking acantholysis in pemphigus. Br J Pharmacol 2020;177:5114–30.

Chernyavsky AI, Arredondo J, Kitajima Y, Sato-Nagai M, Grando SA. Desmoglein versus non-desmoglein signaling in pemphigus acantholysis: characterization of novel signaling pathways downstream of pemphigus vulgaris antigens. J Biol Chem 2007;282:13804–12.

Danilkovitch-Miagkova A. Oncogenic signaling pathways activated by RON receptor tyrosine kinase [published correction appears in Curr Cancer Drug Targets. 2003;3:161]. Curr Cancer Drug Targets 2003;3:31–40.

Egu DT, Schmitt T, Waschke J. Mechanisms causing acantholysis in pemphigus-lessons from human skin. Front Immunol 2022a;13:884067.

Egu DT, Schmitt T, Sigmund AM, Waschke J. Electron microscopy reveals that phospholipase C and Ca2+ signaling regulate keratin filament uncoupling from desmosomes in pemphigus. Ann Anat 2022b;241:151904.

Egu DT, Walter E, Spindler V, Waschke J. Inhibition of p38MAPK signalling prevents epidermal blistering and alterations of desmosome structure induced by pemphigus autoantibodies in human epidermis. Br J Dermatol 2017;177:1612–8.

El Zein N, D'Hondt S, Sariban E. Crosstalks between the receptors tyrosine kinase EGFR and TrkA and the GPCR, FPR, in human monocytes are essential for receptors-mediated cell activation. Cell Signal 2010;22:1437–47.

Fernow I, Tomasovic A, Siehoff-Icking A, Tikkanen R. Cbl-associated protein is tyrosine phosphorylated by c-Abl and c-Src kinases. BMC Cell Biol 2009;10:80.

Frusić-Zlotkin M, Raichenberg D, Wang X, David M, Michel B, Milner Y. Apoptotic mechanism in pemphigus autoimmunoglobulins-induced acantholysis–possible involvement of the EGF receptor. Autoimmunity 2006;39:563–75.

Fuchs M, Kugelmann D, Schlegel N, Vielmuth F, Waschke J. Desmoglein 2 can undergo Ca2+-dependent interactions with both desmosomal and classical cadherins including E-cadherin and N-cadherin. Biophys J 2022;121:1322–35.

Garrod D, Kimura TE. Hyper-adhesion: a new concept in cell-cell adhesion. Biochem Soc Trans 2008;36:195–201.

Garrod DR, Berika MY, Bardsley WF, Holmes D, Tabernero L. Hyper-adhesion in desmosomes: its regulation in wound healing and possible relationship to cadherin crystal structure. J Cell Sci 2005;118:5743–54.

Gaudry CA, Palka HL, Dusek RL, Huen AC, Khandekar MJ, Hudson LG, et al. Tyrosine-phosphorylated plakoglobin is associated with desmogleins but not desmoplakin after epidermal growth factor receptor activation. J Biol Chem 2001;276:24871–80.

Goebeler M, Bata-Csörgő Z, De Simone C, Didona B, Remenyik E, Reznichenko N, et al. Treatment of pemphigus vulgaris and foliaceus with efgartigimod, a neonatal Fc receptor inhibitor: a phase II multicentre, open-label feasibility trial. Br J Dermatol 2022;186:429–39.

Gupta A, Galletti JG, Yu Z, Burgess K, de Paiva CS. A, B, C's of trk receptors and their ligands in ocular repair. Int J Mol Sci 2022;23:14069.

Hariton WVJ, Schulze K, Rahimi S, Shojaeian T, Feldmeyer L, Schwob R, et al. A desmosomal cadherin controls multipotent hair follicle stem cell quiescence and orchestrates regeneration through adhesion signaling. iScience 2023;12:108568.

Heupel WM, Engerer P, Schmidt E, Waschke J. Pemphigus vulgaris IgG cause loss of desmoglein-mediated adhesion and keratinocyte dissociation independent of epidermal growth factor receptor. Am J Pathol 2009;174:475–85.

Heupel WM, Zillikens D, Drenckhahn D, Waschke J. Pemphigus vulgaris IgG directly inhibit desmoglein 3-mediated transinteraction. J Immunol 2008;181:1825–34.

Hiermaier M, Kliewe F, Schinner C, Stüdle C, Maly IP, Wanuske MT, et al. The actin-binding protein α-adducin modulates desmosomal turnover and plasticity. J Invest Dermatol 2021;141:1219–29.e11.

Hofrichter M, Dworschak J, Emtenani S, Langenhan J, Weiß F, Komorowski L, et al. Immunoadsorption of Desmoglein-3-Specific IgG abolishes the blister-inducing capacity of pemphigus vulgaris IgG in neonatal mice. Front Immunol 2018;9:1935.

Hudemann C, Maglie R, Llamazares-Prada M, Beckert B, Didona D, Tikkanen R, et al. Human desmocollin 3–specific IgG antibodies are pathogenic in a humanized HLA Class II transgenic mouse model of pemphigus. J Invest Dermatol 2022;142:915–23.e3.

Iqbal MS, Tsuyama N, Obata M, Ishikawa H. A novel signaling pathway associated with Lyn, PI 3-kinase and Akt supports the proliferation of myeloma cells. Biochem Biophys Res Commun 2010;392:415–20.

Ivars M, España A, Alzuguren P, Pelacho B, Lasarte JJ, López-Zabalza MJ. The involvement of ADAM10 in acantholysis in mucocutaneous pemphigus vulgaris depends on the autoantibody profile of each patient. Br J Dermatol 2020;182:1194–204.

Jensen LJ, Kuhn M, Stark M, Chaffron S, Creevey C, Muller J, et al. STRING 8–a global view on proteins and their functional interactions in 630 organisms. Nucleic Acids Res 2009;37:D412–6.

Joly P, D'Incan M, Musette P. Rituximab for pemphigus vulgaris. N Engl J Med 2007;356:521–2.

Kasperkiewicz M, Ellebrecht CT, Takahashi H, Yamagami J, Zillikens D, Payne AS, et al. Pemphigus. Nat Rev Dis Primers 2017;3:17026.

Kaur B, Kerbrat J, Kho J, Kaler M, Kanatsios S, Cirillo N. Mechanism-based therapeutic targets of pemphigus vulgaris: a scoping review of pathogenic molecular pathways. Exp Dermatol 2022;31:154–71.

Kitajima Y. 150(th) anniversary series: desmosomes and autoimmune disease, perspective of dynamic desmosome remodeling and its impairments in pemphigus. Cell Commun Adhes 2014;21:269–80.

Kugelmann D, Anders M, Sigmund AM, Egu DT, Eichkorn RA, Yazdi AS, et al. Role of ADAM10 and ADAM17 in the regulation of keratinocyte adhesion in pemphigus vulgaris. Front Immunol 2022;13:884248.

Kugelmann D, Rötzer V, Walter E, Egu DT, Fuchs MT, Vielmuth F, et al. Role of Src and cortactin in pemphigus skin blistering. Front Immunol 2019;10:626.

Law CL, Chandran KA, Sidorenko SP, Clark EA. Phospholipase C-gamma1 interacts with conserved phosphotyrosyl residues in the linker region of Syk and is a substrate for Syk. Mol Cell Biol 1996;16:1305–15.

Matada GSP, Das A, Dhiwar PS, Ghara A. DDR1 and DDR2: a review on signaling pathway and small molecule inhibitors as an anticancer agent. Med Chem Res 2021;30:535–51.

Peschard P, Park M. Escape from Cbl-mediated downregulation: a recurrent theme for oncogenic deregulation of receptor tyrosine kinases. Cancer Cell 2003;3:519–23.

Pretel M, España A, Marquina M, Pelacho B, López-Picazo JM, López-Zabalza MJ. An imbalance in Akt/mTOR is involved in the apoptotic and acantholytic processes in a mouse model of pemphigus vulgaris. Exp Dermatol 2009;18:771–80.

Sabbah DA, Hajjo R, Sweidan K. Review on epidermal growth factor receptor (EGFR) structure, signaling pathways, interactions, and recent updates of EGFR inhibitors. Curr Top Med Chem 2020;20:815–34.

Sayar BS, Rüegg S, Schmidt E, Sibilia M, Siffert M, Suter MM, et al. EGFR inhibitors erlotinib and lapatinib ameliorate epidermal blistering in pemphigus vulgaris in a non-linear, V-shaped relationship. Exp Dermatol 2014;23:33–8.

Schinner C, Vielmuth F, Rötzer V, Hiermaier M, Radeva MY, Co TK, et al. Adrenergic signaling strengthens cardiac myocyte cohesion. Circ Res 2017;120:1305–17.

Schmidt E, Kasperkiewicz M, Joly P. Pemphigus. Lancet 2019;394:882–94.

Schmitt T, Hudemann C, Moztarzadeh S, Hertl M, Tikkanen R, Waschke J. Dsg3 epitope-specific signalling in pemphigus. Front Immunol 2023;14:1163066.

Schmitt T, Waschke J. Autoantibody-specific signalling in pemphigus. Front Med (Lausanne) 2021;8:701809.

Schulze K, Galichet A, Sayar BS, Scothern A, Howald D, Zymann H, et al. An adult passive transfer mouse model to study desmoglein 3 signaling in pemphigus vulgaris. J Invest Dermatol 2012;132:346–55.

Shoykhet M, Dervishi O, Menauer P, Hiermaier M, Moztarzadeh S, Osterloh C, et al. EGFR inhibition leads to enhanced desmosome assembly

and cardiomyocyte cohesion via ROCK activation. JCI Insight 2023;8:163763.

Sigmund AM, Winkler M, Engelmayer S, Kugelmann D, Egu DT, Steinert LS, et al. Apremilast prevents blistering in human epidermis and stabilizes keratinocyte adhesion in pemphigus [published correction appears in Nat Commun. 2023;14:665]. Nat Commun 2023;14:116.

Sokol E, Kramer D, Diercks GFH, Kuipers J, Jonkman MF, Pas HH, et al. Large-scale electron microscopy maps of patient skin and mucosa provide insight into pathogenesis of blistering diseases. J Invest Dermatol 2015;135:1763–70.

Spindler V, Eming R, Schmidt E, Amagai M, Grando S, Jonkman MF, et al. Mechanisms causing loss of keratinocyte cohesion in pemphigus. J Invest Dermatol 2018;138:32–7.

Spindler V, Gerull B, Green KJ, Kowalczyk AP, Leube R, Marian AJ, et al. Meeting report - Desmosome dysfunction and disease: Alpine desmosome disease meeting. J Cell Sci 2023;136:jcs260832.

Spindler V, Rötzer V, Dehner C, Kempf B, Gliem M, Radeva M, et al. Peptide-mediated desmoglein 3 crosslinking prevents pemphigus vulgaris autoantibody-induced skin blistering. J Clin Invest 2013;123:800–11.

Sridhar SS, Seymour L, Shepherd FA. Inhibitors of epidermal-growth-factor receptors: a review of clinical research with a focus on non-small-cell lung cancer. Lancet Oncol 2003;4:397–406.

Takano T, Sada K, Yamamura H. Role of protein-tyrosine kinase syk in oxidative stress signaling in B cells. Antioxid Redox Signal 2002;4:533–41.

Tanos B, Pendergast AM. Abl tyrosine kinase regulates endocytosis of the epidermal growth factor receptor. J Biol Chem 2006;281:32714–23.

Trusolino L, Bertotti A, Comoglio PM. MET signalling: principles and functions in development, organ regeneration and cancer. Nat Rev Mol Cell Biol 2010;11:834–48.

Ujiie H, Rosmarin D, Schön MP, Ständer S, Boch K, Metz M, et al. Unmet medical needs in chronic, non-communicable inflammatory skin diseases. Front Med (Lausanne) 2022;9:875492.

Vielmuth F, Radeva MY, Yeruva S, Sigmund AM, Waschke J. cAMP: a master regulator of cadherin-mediated binding in endothelium, epithelium and myocardium. Acta Physiol (Oxf) 2023;238:e14006.

Vielmuth F, Waschke J, Spindler V. Loss of desmoglein binding is not sufficient for keratinocyte dissociation in pemphigus. J Invest Dermatol 2015;135:3068–77.

Walter E, Vielmuth F, Rotkopf L, Sárdy M, Horváth ON, Goebeler M, et al. Different signaling patterns contribute to loss of keratinocyte cohesion dependent on autoantibody profile in pemphigus. Sci Rep 2017;7:3579.

Walter E, Vielmuth F, Wanuske MT, Seifert M, Pollmann R, Eming R, et al. Role of Dsg1- and Dsg3-mediated signaling in pemphigus autoantibody-induced loss of keratinocyte cohesion. Front Immunol 2019;10:1128.

Werth VP, Joly P, Mimouni D, Maverakis E, Caux F, Lehane P, et al. Rituximab versus mycophenolate mofetil in patients with pemphigus vulgaris. N Engl J Med 2021;384:2295–305.

Yamagami J, Takahashi H, Amagai M. Meeting Report: ISID2023 Tokyo Satellite Meeting. International Symposium on Autoimmunity Targeting the Skin. -Pemphigus, Pemphigoid, and Beyond. J Dermatol Sci 2023;112:2–5.

Yin T, Getsios S, Caldelari R, Godsel LM, Kowalczyk AP, Müller EJ, et al. Mechanisms of plakoglobin-dependent adhesion: desmosome-specific functions in assembly and regulation by epidermal growth factor receptor. J Biol Chem 2005;280:40355–63.

Zillikens H, Kasprick A, Osterloh C, Gross N, Radziewitz M, Hass C, et al. Topical application of the PI3Kβ-selective small molecule inhibitor TGX-221 is an effective treatment option for experimental epidermolysis bullosa acquisita. Front Med (Lausanne) 2021;8:713312.